Surrogate-Based Modeling and Sensitivity Analysis of Future European Electricity Spot Market Prices

Julian Quick, Juan Pablo Murcia Leon, Polyneikis Kanellas
Sumanth Yamujala, Kaushik Das, and Matti Juhani Koivisto
Department of Wind and Energy Systems
Technical University of Denmark
Roskilde, Denmark

***Abstract*—Europe is transitioning towards a sustainable energy economy. Planning these future power and energy systems is multifaceted and complex, requiring long-term projections of future electricity market dynamics. The prognostication of future prices is crucial for power system planning, as these prices will drive investments and impact incentives to build and improve new systems. The price of electricity in different regions impacts transmission investment. Energy systems models have high-dimensional output and are expensive to evaluate, leading to unique challenges in managing the uncertainty in model assumptions. This study presents a novel methodology for determining which cost assumptions are most impactful on the output of a detailed model of the European energy system. Because this model is computationally intensive, only a small number of samples are available to us. A multiple-output support vector regression is used as a surrogate of predicted electricity prices timeseries. We find that solar and wind costs are the primary drivers of electricity prices, but natural gas costs generally drive peak electricity prices and those far in the future.**

***Index Terms*—energy systems, sensitivity, uncertainty**

I. Introduction

Europe is transitioning toward a sustainable energy economy with a strong focus on carbon neutrality. The move is intertwined with investments in renewable energy technologies, flexible generators, energy storage, and sector coupling. Energy system planning models, in this context, provide least-cost pathways for decarbonization. They also provide insights into electricity price trajectories, which subsequently influence the investments and profitability of the generation fleet. Prices, and especially price differences between regions, also impact transmission investments. These models are complex and require long-term projections spanning future weather patterns, energy demand, and economic parameters. The outcomes of these models are highly sensitive to the assumptions around commodity prices, technology costs, and carbon taxes. While planning models assume perfect foresight to reduce computational complexities, the uncertainty around the assumptions can be handled by developing various scenarios, with each scenario defining a set of assumptions. Nevertheless, studying diverse scenarios with such complex models is a cumbersome task.

In the European context, energy system models such as Balmorel [1], PyPSA [2], and TIMES [3] have gained prominence as tools for expansion studies. These models are developed using a comprehensive set of equations to optimize the mix of generation technologies while capturing the diverse energy dynamics across European regions. These models often use baseline values of technology cost projections from sources such as the Danish Energy Agency [4]. There is significant uncertainty in these cost projections. These cost uncertainties can impact the projected mix of technologies and concomitant electricity prices. For optimal investment decisions, it is essential to determine the key drivers that influence electricity price trends. The computational intensity of these models is significant, with some scenarios taking more than a day to process.

In this study, we examine the sensitivity of day-ahead spot market electricity prices in an aggressive decarbonization scenario with respect to different technology costs. We present a framework for applying surrogate modeling and sensitivity analysis techniques to energy system planning models like Balmorel to better understand how different technology costs will impact future electricity prices. This framework can be applied to any similar energy systems model. [5] examined the sensitivity of future grid dynamics by assuming different climate, energy, and demand scenarios. [6] examined the sensitivity of a UK energy systems model to technology costs given a single scenario using Monte Carlo sampling with linear regression. [7] studied the same problem using pseudo-Monte Carlo sampling with the method of Morris. In a recent review paper, it is acknowledged that uncertainty in technology is an important aspect of energy systems modeling that deserves more attention [8]. While surrogate methods have been used in the design and analysis of other energy systems models [9], [10], we are not aware of previous publications that apply the proposed timeseries surrogate approach to energy systems.

Sensitivity is quantified on a regional and annual basis. The sensitivity is computed using Monte Carlo simulation, which requires a large number of model samples. One sample of the Balmorel model requires significant computational resources to solve, as it involves an enormous set of linear equations. A single evaluation required approximately two

Submitted to the 23rd Power Systems Computation Conference (PSCC 2024).

days to evaluate when using three 128 GB computational nodes. Due to the expense of the full model, we conduct a surrogate-based sensitivity analysis. A multiple output support vector regression surrogate is employed. The accuracy of the surrogate is confirmed using a leave-one-out (LOO) analysis. Sobol main effects indices are computed using Monte Carlo simulation of the surrogate model. The results of the sensitivity analysis offers several insights into the future dynamics of the European electric grid.

The remainder of this manuscript is structured as follows. Section II presents the surrogate model and sensitivity analysis methodology. Section III presents the Balmorel model and discusses the specific scenario modeled in this study, as well as the ranges of technology costs examined. Section IV presents the results of the LOO and sensitivity analysis. These results are discussed in Section V. Finally, Section VI concludes the study.

II. Methodology

This study presents a surrogate-based sensitivity analysis methodology. The surrogate model is selected to be accurate and memory efficient. This selection includes a detailed continuity analysis, which is supported by a subspace analysis and use of a random forest model.

A. MSVR Surrogate Model

The output of Balmorel is represented using the multiple output support vector regression (MSVR) surrogate model suggested by Bao *et al.* [11]. In the surrogate, a separate MSVR is trained for each region, year, and output examined. The MSVR approach was chosen because it is able to efficiently model thousands of outputs.

Given a set of observed inputs x_{lj}, where l is the sample number and j is the input dimension, the electricity price timeseries is approximated as

$$\boldsymbol{p}(\boldsymbol{x}) \approx \boldsymbol{\beta}\boldsymbol{H}\,, \tag{1}$$

where $\boldsymbol{p}$ is a $n_m \times n_t$ matrix of observed timeseries, $\boldsymbol{\beta}$ is a $n_t \times n_m$ matrix of free parameters, $\boldsymbol{H}$ is a $n_m \times n_m$ matrix constructed from the observations, $\boldsymbol{x}$, using the scikit-learn pairwise kernels function [12], n_t is the number of observed times, and n_m is the number of observed samples of $\boldsymbol{x}$.

The $\boldsymbol{\beta}$ parameters are determined using a linear constrained optimized algorithm to minimize a loss function, L_p. It is defined as

$$L_p(\boldsymbol{\beta}) = R(\boldsymbol{\beta}) + C\sum_{m=1}^{M} L(\boldsymbol{\beta}, \boldsymbol{p}_m)\,, \tag{2}$$

where R is a regularization function and C is a hyperparameter intended to control the model complexity. Larger values of C are designed to yield more complex models, at the risk of overfitting the observed trends. The regularization term, R, is computed as

$$R(\boldsymbol{\beta}) = \frac{1}{2}\mathrm{diag}\left(\beta_{ij}H_{ji}\beta_{ij}\right)\,. \tag{3}$$

.

The loss term $L(\boldsymbol{\beta}, p_{mt})$ is the sum of squared prediction errors, where the root mean squared error (RMSE) is greater than a predefined threshold, ϵ,

$$L(\boldsymbol{\beta}, \boldsymbol{p}_m) = \sum_{m=1}^{M}(u_m^2 - 2\epsilon u_m + \epsilon^2)\cdot I(u_m > \epsilon)\,, \tag{4}$$

where u_m is the RMSE associated with sample m, and I is an indicator function, which returns 1 if the condition inside the parentheses is true, and 0 otherwise. The error function, u_m, is defined as

$$u_m = \left[\frac{1}{n_t}\sum_{t=1}^{n_t}\left(p_{mt} - \beta_{ml}H_{lt}\right)^2\right]^{1/2}\,. \tag{5}$$

When making predictions, the $\boldsymbol{\beta}$ matrix remains constant, and the $\boldsymbol{H}$ matrix is recomputed using Scikit-learn's pairwise kernel, using the convolution of the observed input $\boldsymbol{x}$ and the input prediction points.

B. Leave-One-Out Analysis

One might wonder how many samples are necessary for adequate sensitivity analysis of the energy systems model. The truth is that a perfect sensitivity analysis will require an infinite number of model samples, which is of course impossible. However, mathematical models may be assessed in terms of asymptotic behavior. Any required measure of accuracy can be achieved by adding more samples until an agreeable threshold is reached.

Model accuracy is determined using cross-validation, where the model is blinded to selected samples, then challenged to predict these cases. The difference between the predictions and observations is quantified using the root-mean-squared error (RMSE) between the observed and predicted timeseries.

The hyperparameters of the MSVR surrogate were selected using a leave-one-out (LOO) cross-validation analysis. We selected the best performing model overall, as well as the best performing linear model, to compare the different model characteristics. By best-performing, we mean the model with the lowest mean RMSE across all LOO samples. The asymptotic behavior of the model is examined with respect to the number of model observations by reporting the average RMSE versus sample size, shuffling the sampled data several times.

C. Xgboost Surrogate Model

This study used the extreme gradient boosting algorithm (xgboost) as a secondary surrogate model to verify the results of the MSVR surrogate. Xgboost is a random forest regression model. The xgboost surrogate was trained to predict one electricity price percentile at a time, as opposed to the MSVR surrogate, which predicts the entire timeseries. Unlike MSVR, the xgboost random forest structure does not assume that the approximated function is continuous.

D. Sliced Inverse Regression Analysis

We characterize the developed surrogate models using sliced inverse regression (SIR), a technique that seeks low-dimensional manifolds that can be used for dimension reduction of complex models [13], [14], [15]. Specifically, this yields an eigen decomposition of the input parameter space with respect to the variance in the output.

This is a convenient tool for visualizing data. The data can be plotted against the input dotted with the leading eigenvector, revealing the primary trends of the model. In this work, the sliced inverse regression package [16] is used to compare the behavior of the different surrogate models examined. A continuity analysis is performed to compare the model structure, i.e. to identify which variables cause an increase in a specific electricity price percentile. SIR was used for subspace analysis to identify trends and discontinuities. The xgboost algorithm was used as a neutral reference for identifying trends and discontinuities.

E. Sensitivity Metric Approximation

An MSVR surrogate model is used to estimate the sensitivity of different outputs with respect to different inputs. In this study, sensitivity is primarily quantified via the main Sobol effects index, which is defined as

$$S_i = \frac{\mathrm{Var}_{X_i}\left(\mathbb{E}_{X_{\sim i}}\left(Y|X_i\right)\right)}{\mathrm{Var}(Y)}, \tag{6}$$

where S_i is the main effects Sobol index associated with input i, Var_{X_i} is the variance with respect to input i, and $\mathbb{E}_{X_{\sim i}}$ is the expectation with respect to all inputs except input i.

The main effects Sobol index quantifies the variation in a quantity of interest that can be attributed to variation in the examined input. We select this sensitivity metric because it is widely used and relatively simple to compute.

The main effects index is estimated using the procedure of Saltelli [17]. First, two independent sets of samples are generated, $\boldsymbol{x}^A$ and $\boldsymbol{x}^B$. For each variable, a third set of inputs is constructed as a modification of the first two, to isolate the effects of $X_{\sim i}$ and X_i:

$A \sim \mathcal{U}(-1, 1)$
$B \sim \mathcal{U}(-1, 1)$
evaluate model on sample $f(A)$, $f(B)$
for i in $1, 2, \cdots, \dim(x)$ **do**
  $AB_i = A$.copy()
  $AB_i[i] = B[i]$
  evaluate model on sample $f(AB_i)$
end for

The main effects indices are then approximated as

$$M_i \approx \frac{\mathbb{E}[f(AB_i)f(B)] - \mathbb{E}[f(A)]\mathbb{E}[f(B)])}{\mathbb{E}(A^2) - [\mathbb{E}(A)]^2} \tag{7}$$

where M_i is the main effects index associated with input i and $\mathbb{E}$ denotes the expectation with respect to the uncertain cost multipliers.

III. Application

A. Balmorel Energy Model

In this study, the Balmorel model is used to make projections about potential future energy markets, using the sector coupling structure presented in [18], [19], [20]. The Balmorel model is solved in two stages. The first stage is the capacity expansion optimization, which is used to analyze the energy transitions towards 2050. The capacity expansion optimization is solved at limited temporal granularity (limited number of weeks for each scenario year, 2025, 2035, and 2045 to reduce computational complexity) and aims at finding the needed investment in generation and transmission to meet the electricity, heat and transportation demands for the lowest cost to society. The capacity expansion considers both capital and operational expenditures (CAPEX and OPEX) to optimize the investment decisions. After the capacity expansion optimization is solved, a dispatch run is done, considering all hours of the scenario year, which is equivalent to day-ahead or spot market. The electricity prices presented in this paper are based on this dispatch run, where only the operational and maintenance costs (fixed and variable) play a role, given a generation and transmission capacity per region. While the variable OPEX costs of wind and solar technologies are virtually zero, their fixed OPEX costs (which account for maintenance and labour costs) can impact electricity prices. The different regions of Europe modeled in this study are shown in Fig. 1. The renewable energy generation uses the ERA5 weather data set, with wind modeled as presented in [21]. The technology CAPEX and OPEX are based on a Danish Energy Agency catalogue [4], which provides technology costs for several years. These projections are are all used in Balmorel for the different years.

The results associated with the baseline model are shown in Fig. 2. The baseline model reflects the EU's decarbonization initiatives in terms of variable renewable energy (VRE) dominant electricity generation, electrification of transport and heat sectors, and production of green hydrogen. The transition is expected to result in more than a twofold increase in electricity demand by 2045 compared to 2025, as shown in Fig. 2(a). Towards 2045, VRE technologies, especially wind and solar, dominate the generation mix, while some of the required flexibility in the electricity sector is contributed by combined heat and power (CHP), thermal, and hydro generators, as illustrated in Fig. 2(b). The fossil-fuel driven heat and hydrogen sectors will transition to electricity as a primary source. Starting from 2035, the major portion of heating demand will be met by heat pumps. Also, electrolyzer operations will cater to heating needs as shown in Fig. 2(c). Apart from controllable generators, VRE uptake is driven by the energy storage operations across all sectors, as depicted in Fig. 2(d). Electric vehicles operating in grid-to-vehicle and vehicle-to-grid modes result in deferred investments in short-term energy storage, such as batteries.

The uncertainty in the underlying CAPEX and OPEX assumptions is modeled by multiplying the technology cost

Fig. 1. A map depicting the different European regions modeled in this study. DK1-DK2, NO1-NO5, and SE1-SE4 represent the existing electricity market bidding zones of Denmark, Norway, and Sweden. Germany (DE) is split into four regions – east, west, north and south. BE, EE, FIN, FR, LI, LV, NL, PL, and UK represent Belgium, Estonia, Finland, France, Lithuania, Latvia, Netherlands, Poland, and the United Kingdom, respectively.

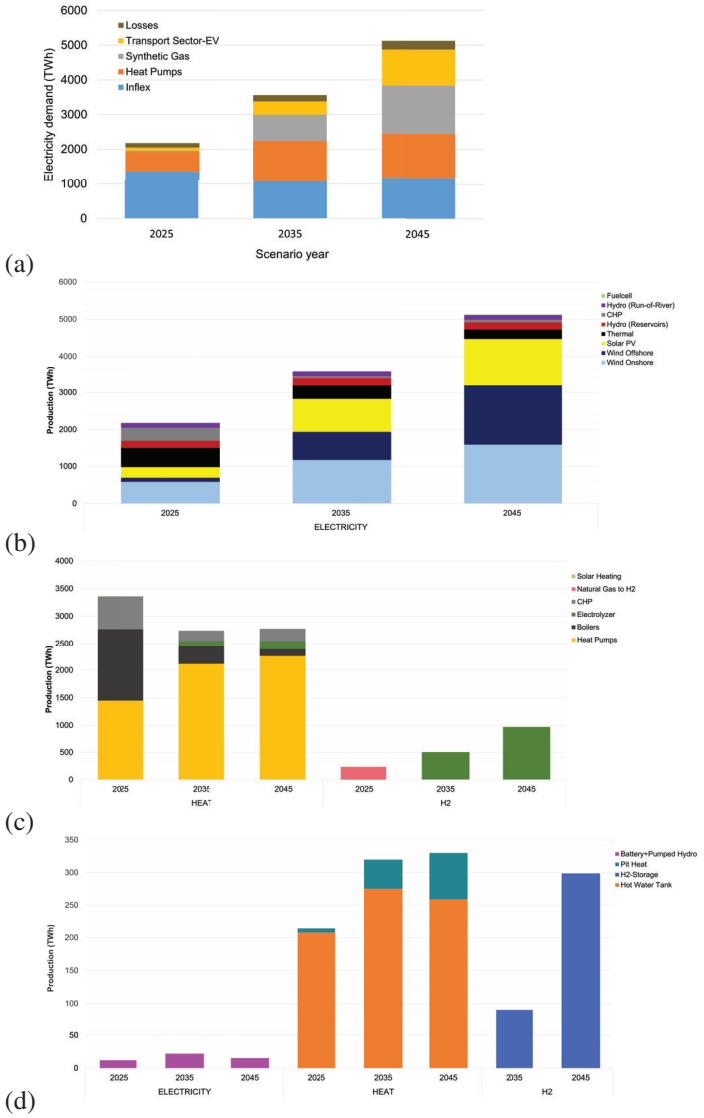

Fig. 2. Simulation results associated with the baseline technology costs model: (a) Sector-wise electricity demand. (b) Technology-wise electricity production. (c) Heat and hydrogen production. (d) Energy storage dispatch for each scenario year. These are the aggregated results across all regions.

evolution for both CAPEX and OPEX by a constant cost factor across time. The multiplicative factors associated with each technology cost are shown in Table I. A multiplicative factor of one corresponds to the baseline case presented in Fig. 2, it assumes the cost projections originally made by the Danish Energy Agency.

An MSVR surrogate model was trained to predict the electricity prices as a function of the uncertainty cost factors using 34 model evaluations. The first 12 model evaluations were selected by changing one input at a time. These evaluations were also used to internally inspect the Balmorel configuration used in this study. The remaining 22 samples were randomly selected using the Latin hypercube sampling method [22]. Individual MSVR models were trained to predict each region- and scenario-year-specific electricity price timeseries.

The inputs and outputs are normalized in a preprocessing step. The inputs are normalized to range from 0 to 1 using the scikit-learn standard scaler, which applies a linear transformation. The price timeseries are normalized from 0 to 1 using the scikit-learn quantile transformer, which ensures that the transformed output follows a uniform distribution. This step encodes the observed range of time-specific prices. This time-specific scaling avoids the complication of variability due to seasonal effects. We used 100 quantiles when normalizing the observed electricity prices. When performing Monte Carlo sampling of the surrogate model, we used 100,000 samples to compute the Sobol main effects index.

TABLE I
LOWER AND UPPER BOUNDS OF COST MULTIPLIERS CONSIDERED IN THE ENERGY SYSTEM SIMULATION

Parameter	Lower Bound	Upper Bound
Onshore Wind Cost	0.8	1.2
Offshore Wind Cost	0.7	1.3
Solar PV Cost	0.8	1.2
Natural Gas Price	1	10
CO2 Bond Price	0.8	1.2
Heat Pump Costs	0.8	1.2
Electrolyzer Cost	0.8	1.2

B. Leave-One-Out Hyperparameter Grid Search

A LOO analysis was performed to select the hyperparameters of the surrogate model. The LOO error is computed by leaving one sample out of the data set at a time. The model, trained with this slightly reduced data set, is used to predict the electricity prices associated with the unseen data point. To avoid computations that would otherwise have been too burdensome, we limit our analysis to the United Kingdom in 2045 during the LOO analysis.

A grid search was conducted to characterize the model input. The model parameters considered are shown in Table II. All combinations of these hyperparameters were evaluated using the LOO cross validation score. The kernel, $k(\boldsymbol{x}_i, \boldsymbol{x}_j)$, is the function that defines the construction of the $\boldsymbol{H}$ matrix. The length scale, γ, controls the width of the radial basis function (RBF) and Laplace kernels, and influences the polynomial kernel. The complexity parameter, C, controls the influence of the regularization term, R. The ϵ parameter determines the minimum acceptable error. Note that the degree parameter is only applicable to the polynomial kernel.

TABLE II
RANGE OF PARAMETERS CONSIDERED IN THE GRID SWEEP LOO ANALYSIS.

Parameter	Swept Values
kernel	polynomial, Laplace, RBF
γ	0.001, 0.05, 0.1, 0.2, 0.4, 0.8, 1, 5
C	1, 10, 10^2, 10^3, 10^4, 10^5, 10^{10}, 10^{20}
ϵ	10^{-12}, 10^{-2}, 10^{-1}, 1, 5, 10
degree	1, 2, 3, 4
tolerance	10^{-1}, 10^{-3}, 10^{-5}, 10^{-8}, 10^{-12}

IV. RESULTS

The surrogate model was created using the 34 sampled points. The first 12 points were selected by setting individual values to their upper and lower bounds, keeping the rest at the baseline, for verification purposes. The remaining 22 points were selected using Latin hypercube sampling. The surrogate model accuracy is assessed in Section IV-A. The sensitivity analysis is performed in Section IV-B.

A. Leave-One-Out Analysis

LOO analysis is performed to select model hyperparameters. In this analysis, the model is blinded to one sampled model realization at a time, and is challenged to predict the price timeseries associated with the missing point. Additionally, the full model (trained with all the data, including the LOO point) is used for prediction. The RMSE of the predicted timeseries is compared to the real Balmorel output to quantify the error in each region-time. After a detailed hyperparameter grid search, we selected a Laplacian kernel to minimize the mean of the LOO RMSE errors. This is contrasted to a linear kernel, selected as the model with a polynomial degree of 1 that yields the lowest mean LOO RMSE across all LOO points. This happens to set $\gamma = 1$, which corresponds exactly to a linear kernel. The mean and maximum of the region-time LOO errors are shown in Fig. 3. The y-axis shows errors associated with models blinded to each LOO sample. The x-axis shows errors associated with the full model, which is not blinded to any of the true Balmorel samples. Although the Laplacian model yields a maximum test RMSE of about 30 Euros/MWh, which is one of the best-performing parameter configurations tested, it is not very much lower than the bulk of the test errors. The linear model has a slightly larger mean RMSE than the Laplacian model, though it yields a slightly lower maximum RMSE across all LOO cases. The distributions of the linear and nonlinear model RMSE errors (across the individual LOO samples) are visualized in Figure 4. The two models again appear to be quite similar. They both yield essentially the same errors in the worst LOO case. The bulk of the observed errors have RMSE less than about 20 Euro/MWh.

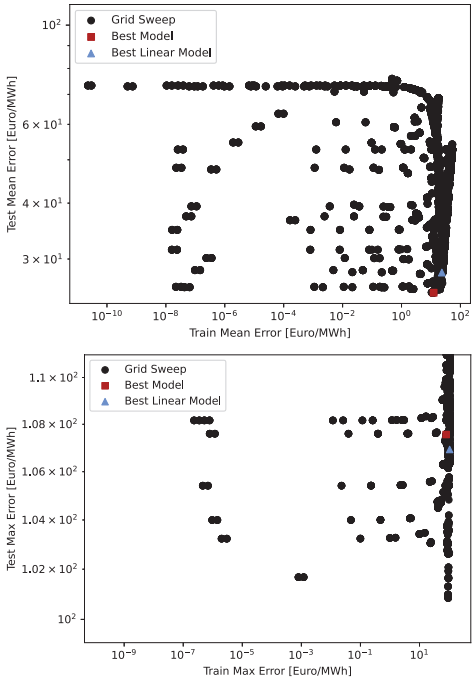

Fig. 3. Results of the parameter grid sweep. The trade-offs between the training and testing error are visualized. The red point shows the Laplacian kernel, which was selected to minimize the RMSE associated with the LOO analysis. The blue point shows the linear kernel, which was selected for model simplicity.

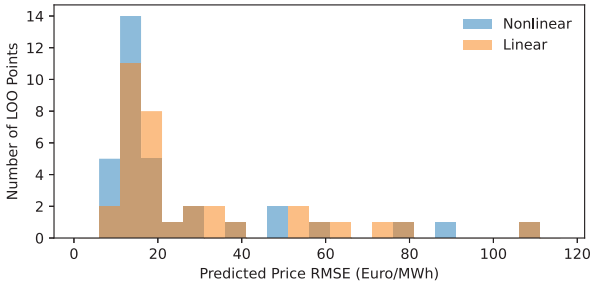

Fig. 4. Observed LOO RMSE for the linear and nonlinear kernels selected in Figure 3.

The selected model hyperparameters were used to train a

production surrogate. As validation, the timeseries prediction associated with these hyperparameters was compared to an unseen region-year, using the previously described LOO analysis. One of the LOO timeseries is visualized in Fig. 5. Both the linear and nonlinear models match the observations to a reasonable degree. In this case, the linear model matched the LOO data better than the nonlinear model.

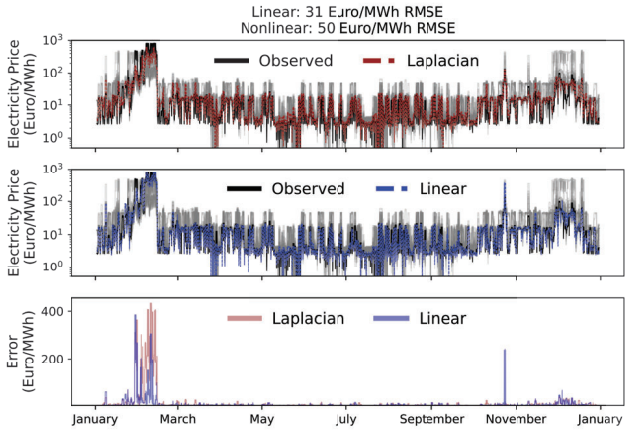

Fig. 5. The prediction of the leave-one-out model for the UK region in 2024 compared to the excluded data. The top panel shows the results associated with the laplacian kernel. The middle panel shows the results associated with the linear kernel. The bottom panel compares the absolute errors associated with both kernels. The grey lines show the CDFS associated with each sampled observation.

The economics of energy systems are often quantified using a CDF of predicted energy prices. Thus, we compare the observed CDF of three selected LOO cases to the predictions associated with the linear and Laplacian models in Fig. 6. Both models yield the largest RMSE when predicting LOO case 30, shown in the left panel. The linear and nonlinear models are very similar in this case, and the associated RMSEs only differ by 1 Euro/MWh. The middle and right panels show cases that highlight the different predictions between the linear and nonlinear models.

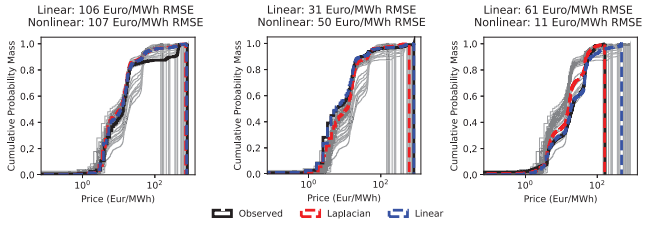

Fig. 6. CDFs associated with the predictions of the LOO analysis compared to the excluded data. The left panel shows the case associated with largest RMSE in both the linear and Laplacian kernels. The middle and right panels show selected cases. The grey lines show the CDFS associated with each sampled observation.

The asymptotic behavior of the RMSE is examined by performing the LOO with different sample sizes, reporting the mean RMSE across several shuffles of the data. The results are shown in Figure 7. While adding more samples will undoubtedly refine the surrogate model and lower the examined error metric, it is clear that hundreds, thousands, or even millions of model evaluations may be necessary to satisfy an extreme RMSE tolerance, e.g., one Euro per megawatt-hour. The 34 samples used in this analysis appear to have captured the main trends in the model. As a sanity check, we internally ran the model with 58 samples, which yielded similar sensitivity analysis results with the same conclusions presented in the proceeding sections.

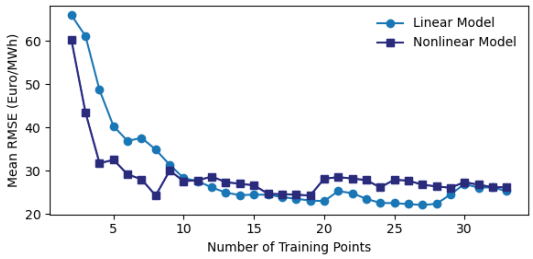

Fig. 7. Mean LOO RMSE plotted as a function of the number of samples used to train the selected linear and nonlinear models.

Based on this analysis, it is a matter of ambiguity whether the Laplacian model is truly a better predictor than the linear model. While the Laplacian model yields a slightly lower mean RMSE across all LOO cases, there are many cases where the linear model outperforms the nonlinear model.

B. Sensitivity Analysis

This study focuses on sensitivity analysis that is relevant to decision makers by quantifying the sensitivity of different electricity prices with respect to different technology costs. This necessitates a choice between the linear and Laplacian models, so that the analysis results can be properly interpreted. The linear surrogate captures first-order effects, imposing a linear input-output structure, while the Laplacian model conforms perfectly to training data, imposing a nonlinear continuous structure to match all observations. We contrast the two modeling choices by sampling the MSVR model with the selected linear and Laplacian kernels, comparing the results to those predicted by xgboost regressors trained on selected price percentiles. The xgboost model uses a decision tree structure to predict model outputs. This avoids any assumption of continuity, making it a useful comparison to the MSVR models, which assume continuity.

In Fig. 8, predicted and observed electricity price percentiles of a selected region-year are compared along a subspace computed by applying SIR to the Monte Carlo samples of the surrogate. This is sometimes referred to as a "shadow plot." The active subspace directions, plotted as orange bars, reveal the direction in the seven-dimensional parameter space that is associated with the most variation in the examined quantities of interest. While large electricity prices (i.e., the 95th percentile) are generally increased when increasing natural gas costs, lower electricity prices (i.e., the 20th percentile) are

slightly reduced when natural gas prices are increased. This is likely due to large electricity prices driving early investments in renewables and transmission lines. The linear model yields an active direction that separates the observed 80th percentile prices into a clear discontinuity. The combination of the linear model and selected preprocessing has essentially smoothed out this discontinuity. On the other hand, the Laplacian model yields an active direction that orders the points into a cloud of descending values, without a clear discontinuity.

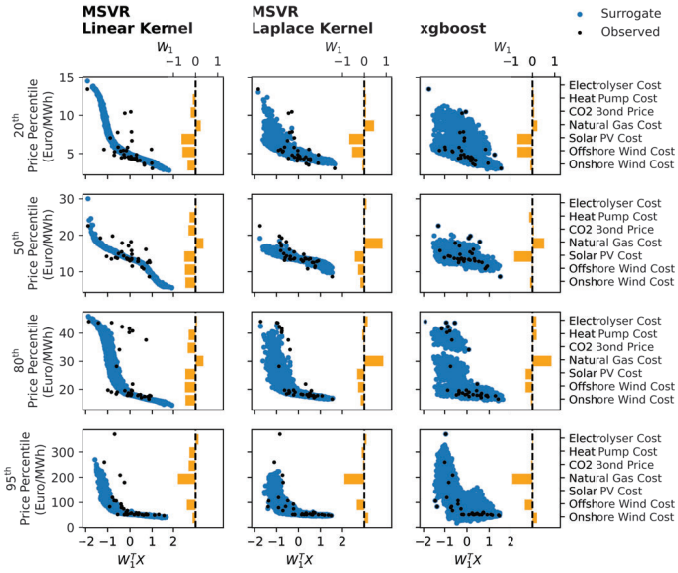

Fig. 8. Surrogate predictions are compared to a leave-one-out sample from SE1 year 2045. Different percentiles of the electricity price in this region-year in Sweden are predicted based on three different models. The first two models (linear and Laplacian) refer to the MSVR surrogates, which model the entire timeseries. The third model, xgboost, is trained to directly predict the examined percentile, using the aforementioned leave-one-out approach. The leading eignvector resulting from SIR analysis of the surrogate model samples is denoted as W_1.

The leading eigenvector discovered by SIR quantifies the importance of the different inputs with respect to the variance in an examined quantity of interest. While this does not include additional eigenvectors, and is not a widely used sensitivity metric, the presented SIR analysis results are generally aligned with the trends revealed by the full Sobol effects sensitivity analysis presented in Fig. 9 and in the Appendix in Fig. 11. High electricity prices are driven by natural gas costs. Solar and onshore/offshore wind costs drive the majority of electricity prices, particularly in 2025 and 2035; and natural gas costs drive peaks in electricity prices. Norway prices stand out as more sensitive to offshore wind costs and less sensitive to natural gas costs than other regions. The electricity price in France stands out as being particularly sensitive to solar photovoltaic costs. There is a complex shift around the 80th electricity price percentile, where peak pricing starts to take effect. The sensitivity of natural gas costs tends to form a trough around higher electricity prices in later years, indicating that other factors will drive this sometimes narrow range of electricity prices. There is some sensitivity to the electrolyzer, heat pump, and CO2 bond costs; but these are all clearly secondary factors, given the assumed range of variation in costs.

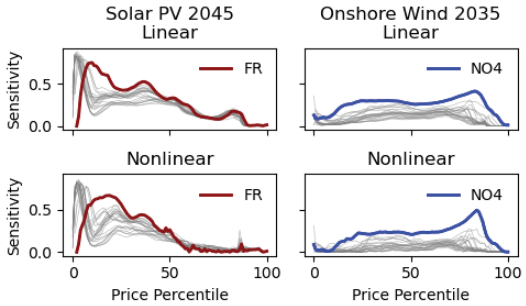

Fig. 9. Main Sobol effects index associated with solar and onshore wind costs. The results of the selected linear and nonlinear kernels are compared in the upper and lower rows. The left column shows the sensitivity of 2024 prices with respect to solar technology costs and the right column shows the sensitivity of 2035 prices with respect to onshore wind technology costs. France and Norway region 4 are highlighted as outlier regions. The grey lines shows the results associated with all other regions. The price sensitivity is reported as a function of the price percentile.

While the electrolyzer, heat pump, and CO2 bond costs were not found to be significant when examining the SIR leading eigenvector, the Sobol main effects analyses indicate that electricity prices around the 80th percentile show some sensitivity to these costs. Most notably, the linear and Laplacian models report different trends in the sensitivity of low- to medium-price electricity percentiles with respect to natural gas costs. This is highlighted in Fig. 10.

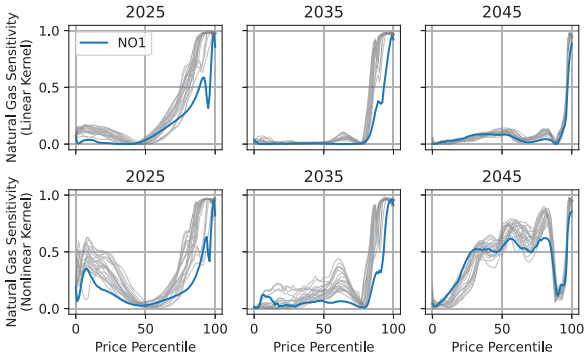

Fig. 10. Sobol main sensitivity of different electricity price percentiles with respect to the cost of natural gas. The different columns correspond to different years. The top row shows results associated with the linear kernel and the bottom row shows results associated with the nonlinear kernel. Results associated with different regions are shown as grey lines. The NO1 region is highlighted as an outlier.

V. Discussion

The observed difference in sensitivity metrics approximated using the linear and nonlinear models is likely due to discontinuities associated with transmission line construction. Construction of these lines is based on differences in region-specific electricity prices. Early transmission line construction

can have profound impacts when examining long-term changes in electricity prices. While the specific prices predicted by the Laplacian model are likely imperfect predictions, the goal of our analysis is to quantify the sensitivity of an aggregate of the predicted electricity price timeseries. There will likely be discontinuities in future electricity market prices, so we select the Laplacian model as being most representative of realistic market dynamics for the purposes of our sensitivity analysis. While the reported Sobol indices quantify the variance attributed to each model input, they do not offer information regarding the direction of variation, or if the output is smooth. The SIR model is used to compliment the Sobol index analysis, giving the reader an idea of the direction of output price variation associated with variation in the technology costs, as well as the smoothness of the predicted prices with respect to these costs.

Observing discontinuities in the subspace analysis initially raised some alarm bells, as discontinuities can be a significant challenge to nonlinear kernels. After re-examination of the LOO analysis, we determined that the discontinuities predicted by xgboost were likely the results of spikes in electricity prices that were captured by the nonlinear model, as noted in the LOO analysis. It seems likely that these discontinuities are the result of transmission lines being built between regions. The construction of these lines is driven by price differences across regions. The cost of natural gas likely drives peak prices in each region, which in turn drives transmission line construction, leading to big discontinuities in 2045.

This analysis identified three outlier regions when considering the sensitivity of each electricity price percentile with respect to different technology costs. The FR region has a relatively large solar resource, which likely caused the larger sensitivity to solar costs identified in Figure 9. The NO4 region, highlighted in the same figure, yields a large sensitivity to onshore wind costs. This is likely due to the large rural areas available to develop wind farms, which generally have a relatively large wind resource. In Figure 10, the NO4 region is highlighted as being less sensitive to natural gas costs than other regions. This is likely due to the large hydro-electric storage facilities in the region, as well as the availability of several neighboring regions to connect with transmission lines.

The large spikes in the electricity market are predicted based on supply and demand. These occur during periods, usually in winter, when there is a lot of demand for electricity but not enough supply from renewable sources, due to weather conditions. These large spikes are highly undesirable for society.

VI. Conclusions

This analysis presents the construction of a surrogate for sensitivity analysis of electricity prices predicted by the Balmorel energy system model, yielding insights into what technology costs will drive future electricity markets under an aggressive decarbonization scenario. The cost of natural gas is the biggest driver of high electricity prices, and becomes the dominant driver of electricity prices far into the future. Wind and solar are the biggest drivers of most electricity prices, particularly during the early years of the decarbonization transition.

The results of the Balmorel model are highly nonlinear and, as seen in our analysis, exhibit extreme discontinuities. The model is complex and computationally intensive, and the 34 samples used in this analysis required significant computational and human resources. We selected an MSVR surrogate model to represent the complexity of the high-dimensional output.

We closely examined linear and nonlinear models during this analysis, and ultimately selected the nonlinear kernel, because it captured sudden electricity price discontinuities, which are crucial to the sensitivity analysis results. In other settings, the linear model may be more appropriate, as the spikes in electricity prices are difficult for the nonlinear model to reliably predict. However, in our analysis, it is most important that the trends in electricity prices accurately reflect the true sensitivity of the model, which the nonlinear kernel accomplishes best. While the nonlinear and linear models yielded similar sensitivity analysis results concerning solar and onshore wind costs, both predicting outliers in the FR and NO4 regions, there is a significant difference between the different models' analysis results when examining sensitivity to natural gas costs.

In future work, we plan to address limitations of this analysis by drastically increasing the sample size, accounting for more realistic weather forecasts with different potential weather conditions, and analyzing different scenarios, in addition to parameter uncertainties.

References

[1] F. Wiese, R. Bramstoft, H. Koduvere, A. P. Alonso, O. Balyk, J. G. Kirkerud, Å. G. Tveten, T. F. Bolkesjø, M. Münster, and H. Ravn, "Balmorel open source energy system model," *Energy strategy reviews*, vol. 20, pp. 26–34, 2018.

[2] J. Hörsch, F. Hofmann, D. Schlachtberger, and T. Brown, "PyPSA-Eur: An open optimisation model of the european transmission system," *Energy strategy reviews*, vol. 22, pp. 207–215, 2018.

[3] K. Vaillancourt, M. Labriet, R. Loulou, and J.-P. Waaub, "The role of nuclear energy in long-term climate scenarios: An analysis with the world-TIMES model," *Energy Policy*, vol. 36, no. 7, pp. 2296–2307, 2008.

[4] Danish Energy Agency, "Technology data for generation of electricity and district heating," Website, 2023, accessed: June 2023. [Online]. Available: https://ens.dk/en/our-services/projections-and-models/technology-data/technology-data-generation-electricity-and

[5] H. Bloomfield, D. Brayshaw, A. Troccoli, C. Goodess, M. De Felice, L. Dubus, P. Bett, and Y.-M. Saint-Drenan, "Quantifying the sensitivity of european power systems to energy scenarios and climate change projections," *Renewable Energy*, vol. 164, pp. 1062–1075, 2021.

[6] S. Pye, N. Sabio, and N. Strachan, "An integrated systematic analysis of uncertainties in uk energy transition pathways," *Energy Policy*, vol. 87, pp. 673–684, 2015.

[7] W. Usher, "The value of global sensitivity analysis for energy system modelling," *University College London*, 2015.

[8] M. Fodstad, P. C. del Granado, L. Hellemo, B. R. Knudsen, P. Pisciella, A. Silvast, C. Bordin, S. Schmidt, and J. Straus, "Next frontiers in energy system modelling: A review on challenges and the state of the art," *Renewable and Sustainable Energy Reviews*, vol. 160, p. 112246, 2022.

[9] W. Du, H. E. Garcia, W. R. Binder, and C. J. Paredis, "Value-driven design and sensitivity analysis of hybrid energy systems using surrogate modeling," in *2014 International Conference on Renewable Energy Research and Application (ICRERA)*. IEEE, 2014, pp. 395–400.
[10] J. Jiang, H. Yu, G. Song, J. Zhao, K. Zhao, H. Ji, and P. Li, "Surrogate model assisted multi-criteria operation evaluation of community integrated energy systems," *Sustainable Energy Technologies and Assessments*, vol. 53, p. 102656, 2022.
[11] Y. Bao, T. Xiong, and Z. Hu, "Multi-step-ahead time series prediction using multiple-output support vector regression," *Neurocomputing*, vol. 129, pp. 482–493, 2014.
[12] F. Pedregosa, G. Varoquaux, A. Gramfort, V. Michel, B. Thirion, O. Grisel, M. Blondel, P. Prettenhofer, R. Weiss, V. Dubourg *et al.*, "Scikit-learn: Machine learning in python," *the Journal of machine Learning research*, vol. 12, pp. 2825–2830, 2011.
[13] K.-C. Li, "Sliced inverse regression for dimension reduction," *Journal of the American Statistical Association*, vol. 86, no. 414, pp. 316–327, 1991.
[14] P. G. Constantine, *Active subspaces: Emerging ideas for dimension reduction in parameter studies*. SIAM, 2015.
[15] J. Quick, R. N. King, M. T. H. de Frahan, S. Ananthan, M. Sprague, and P. E. Hamlington, "Field sensitivity analysis of turbulence model parameters for flow over a wing," *International Journal for Uncertainty Quantification*, vol. 12, no. 1, 2022.
[16] J. Loyal, "sliced: A python package for sufficient dimension reduction techniques," https://github.com/joshloyal/sliced, 2018, florida State University, Tallahassee, FL.
[17] A. Saltelli and I. M. Sobol, "About the use of rank transformation in sensitivity analysis of model output," *Reliability Engineering & System Safety*, vol. 50, no. 3, pp. 225–239, 1995.
[18] J. Gea-Bermúdez, I. G. Jensen, M. Münster, M. Koivisto, J. G. Kirkerud, Y.-k. Chen, and H. Ravn, "The role of sector coupling in the green transition: A least-cost energy system development in northern-central europe towards 2050," *Applied Energy*, vol. 289, p. 116685, 2021.
[19] P. Swisher, J. P. M. Leon, J. Gea-Bermúdez, M. Koivisto, H. A. Madsen, and M. Münster, "Competitiveness of a low specific power, low cut-out wind speed wind turbine in north and central europe towards 2050," *Applied Energy*, vol. 306, p. 118043, 2022.
[20] J. Gea-Bermúdez, R. Bramstoft, M. Koivisto, L. Kitzing, and A. Ramos, "Going offshore or not: Where to generate hydrogen in future integrated energy systems?" *Energy Policy*, vol. 174, p. 113382, 2023.
[21] J. P. Murcia, M. J. Koivisto, G. Luzia, B. T. Olsen, A. N. Hahmann, P. E. Sørensen, and M. Als, "Validation of european-scale simulated wind speed and wind generation time series," *Applied Energy*, vol. 305, p. 117794, 2022.
[22] W.-L. Loh, "On latin hypercube sampling," *The annals of statistics*, vol. 24, no. 5, pp. 2058–2080, 1996.

VII. Appendix

The sensitivity of the electricity price was quantified across three years and all the regions shown in Fig. 1 on a percentile basis. The full results of the sensitivity analysis are shown in Fig. 11. The columns are divided by choice of kernel (linear or Laplacian), and further subdivided by the year analyzed. The sensitivity of the electricity price, with respect to each of the seven technology costs examined, is shown as a function of the electricity price percentile associated with each region-year. These sensitivities are represented as circles filled by the national flag of the associated region. Note that different regions associated with the same country (e.g., DK1 and DK2) are represented with identical markers.

The linear and nonlinear kernels result in similar sensitivity trends, with the notable exception of natural gas sensitivity, as discussed in the main text. Both models predict that CO2 bond prices have noticeable sensitivity in 2025. The linear model indicates that there is some sensitivity with respect to heat pump costs in later years. The Laplacian model indicates similar trends with respect to the heat pump cost.

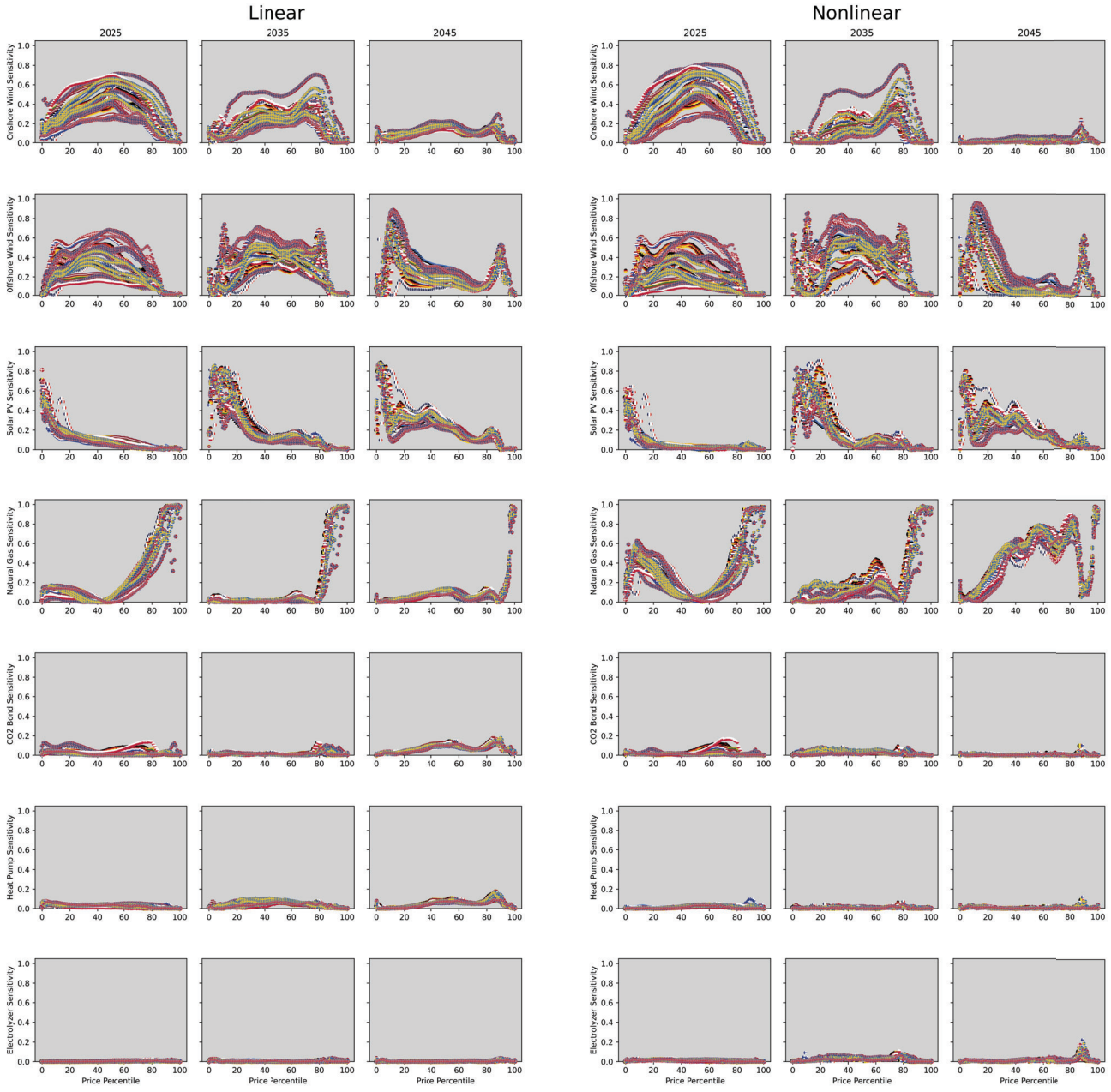

Fig. 11. Main Sobol effects index (y-axis) associated with different electricity price percentiles (x-axis) for different regions (markers) and years (columns), using MSVR. The three leftmost columns are associated with the linear kernel. The three rightmost columns are associated with the Laplacian kernel.